# Modeling and Experimental Characterization of a High-Field, High-Charge L-Band Photoinjector

**Chengkun Huang[1], Xueying Lu[2,3], Omkar Ramachandran[2], Gaurab Rijal[2]**

1. Los Alamos National Laboratory (LANL)
2. Northern Illinois University (NIU)
3. Argonne National Laboratory (ANL)

AAC 26

# Acknowledgments

- A. Alexander (LANL)
- Gongxiaohui Chen (ANL)
- D. A. Dimitrov (LANL)
- Alex Ody (ANL)
- John Power (ANL)
- Omkar Ramachandran (NIU)
- Gaurab Rijal (NIU)
- E. I. Simakov (LANL)
- Gaoxue Wang (LANL)
- Eric Wisniewski (ANL)

This research was supported by:
**Los Alamos National Laboratory (LANL):** LDRD 20230011DR
**Northern Illinois University (NIU):** DE-SC0021928,DE-SC0024445.
**Argonne National Laboratory (ANL):** DE-AC02-06CH11357

# Outline

- Goal:
  - Understanding of $Cs_2Te$ photocathode operation in a high-field photocathode gun
- Approach:
  - Modeling: DFT + Monte-Carlo + thin-film optical interference
  - Experimental benchmarking at the Argonne Wakefield Accelerator, using an L-band (1.3 GHz) high-field $Cs_2Te$ photogun
- Application:
  - High-brightness beam generation
  - High-gradient photoguns (e.g., normal-conducting photoguns at other frequencies, such as C- or X-band, water-cooled or cryogenic; SRF guns)

# Understanding semiconductor photocathode in gun operating conditions

- **High-field operation** is of advantage for increasing beam brightness but also has inherent complexity
  - Suitable photocathode materials (e.g., $Cs_2Te$)
  - Mitigation design and optimization
- Adequate models and knowledge of material properties to help guide the photocathode and gun design
  - No suitable existing models for **high-field photoemission**, some include Schottky and space-charge effects in emission
  - Unknown or uncertain material properties (e.g., **optical constants** for $Cs_2Te$)

PITZ $Cs_2Te$ gun

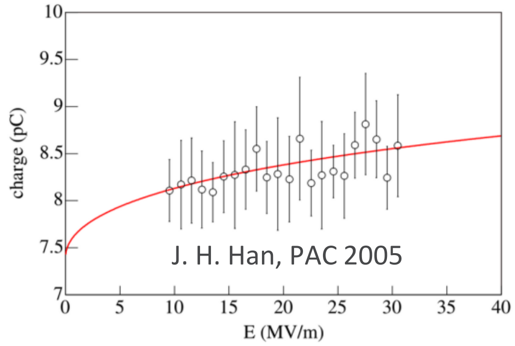


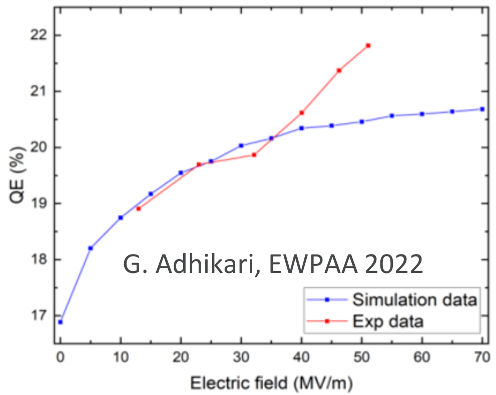

# Emission models

Fowler–Dubridge $$QE_F = \eta(h\upsilon - \Phi_\omega)^2,$$

Spicer $$QE_s = \frac{(h\upsilon - \Phi_\omega)^{1.5}}{(h\upsilon - \Phi_\omega)^{1.5} + \gamma}.$$

Jensen $$QE_J = \frac{(1 - R_\omega)\sqrt{1 + \frac{h\upsilon - \Phi_\omega}{E_a}}}{2(p_0 + 1)\left(1 + \frac{E_a}{h\upsilon - \Phi_\omega}\right)^2}.$$

## Schottky effect

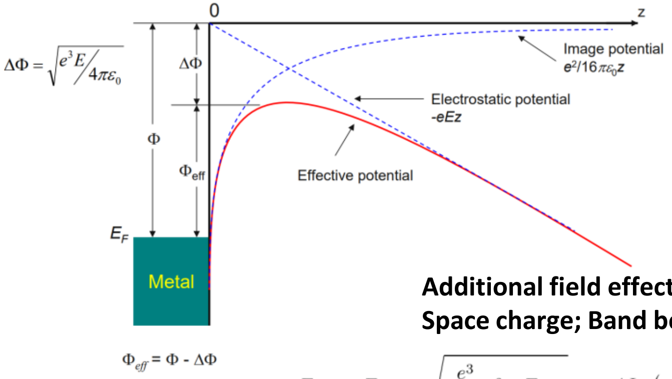


**Additional field effects: Field enhancement; Space charge; Band bending**

$$E_A = \kappa E_{A,0} - \sqrt{\frac{e^3}{4\pi\epsilon_0}\beta_{ph} E_{emit}}\,. \qquad \Delta\Phi_f(r_\perp, t) = \sqrt{\frac{q^3}{4\pi\varepsilon_0}\left[E_{rf}(r_\perp, t) + E_{sc}(r_\perp, t)\right]}$$

## Optical interference effect

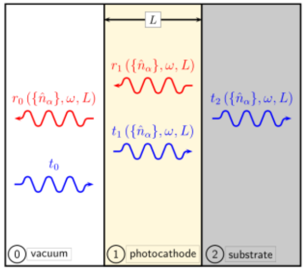


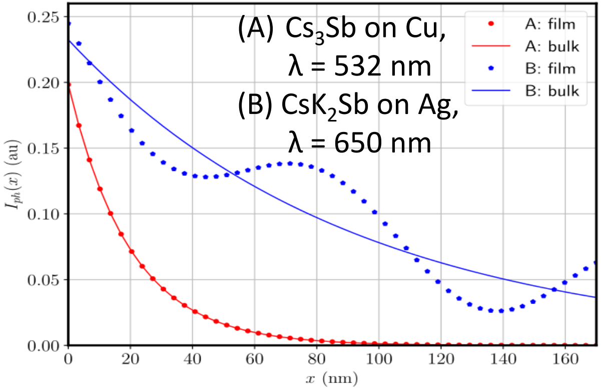

# Moment model and Monte-Carlo modeling

- Moment model for photoemission

Moments: $M_n(k_j) \equiv \langle k_j^n \rangle$ absorption (A), transport (T), emission (E)

$$M_n(k_j) = (2\pi)^{-3} \int d^3k k_j^n \times \mathbb{E} \times \mathbb{T} \times \mathbb{A}$$

for a semi-infinite photocathode

QE expressed as averages over electron energies:

$$QE = (1 - R(\omega)) \frac{\int_{E_a}^{\hbar\omega - E_g} dEE \int_{\sqrt{E_a/E}}^{1} duD(Eu^2)uf_{si}(\omega, E, u)}{2\int_0^{\hbar\omega - E_g} dEE \int_0^1 du}$$

Absorption and transport: thin film photocathode

$$f_{tf}(\omega,\ E,\ \cos(\theta)) = \frac{\int_0^L |E_{ph}(x)|^2 e^{-x/(\lambda(E)\cos(\theta))} dx}{\int_0^L |E_{ph}(x)|^2 dx}$$

- Monte-Carlo approach is suitable for detailed transport process modeling

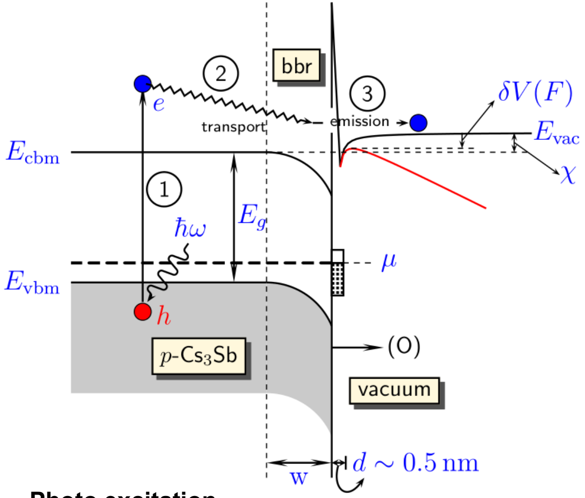


1. **Photo excitation**
2. **Charge transport**
3. **Surface emission**

# Informing emission model with parametrized MC transport

- We utilize a Monte Carlo simulation model and adapt the simulations for $Cs_2Te$ semiconductor cathodes.
- Electronic properties from DFT calculation (as well as from literature/experiment)

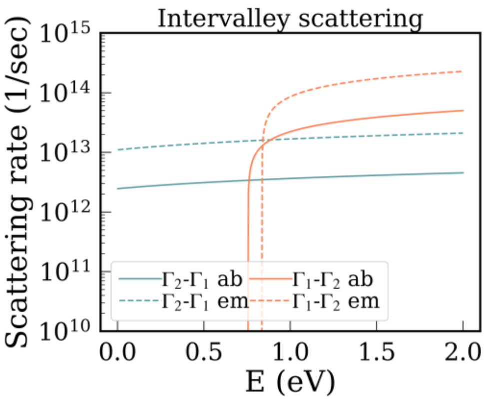


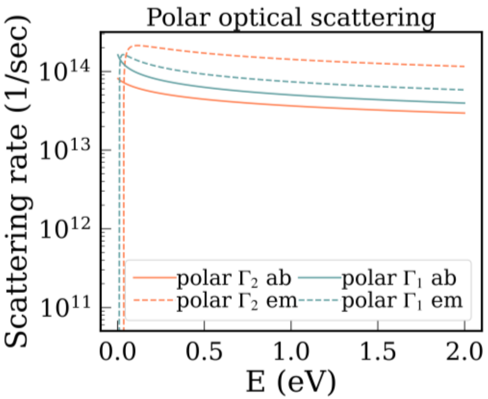


Table 1: Parameters for the $Cs_2Te$ transport simulation. *Experimental value [4].

| Parameters | Value |
|---|---|
| Band gap $E_g$ | 3.3 eV* |
| $\Gamma_1$ valley effective mass ($m_1^*$) | 0.27 $m_0$ |
| $\Gamma_2$ valley effective mass ($m_2^*$) | 0.7 $m_0$ |
| $\Gamma_1 - \Gamma_2$ splitting energy $E_s$ | 0.796 eV |
| Phonon energy $E_{ph}$ (estimate) | 0.01 eV |
| Deformation constant $D_i$ (estimate) | $10^{11}$ eV/m |
| Dielectric constant $\epsilon_s$ | 10.3 $\epsilon_0$ |
| High frequency dielectric constant $\epsilon_\infty$ | 4.3 $\epsilon_0$ |
| Density $\rho$ | 3.99 g/cm$^3$ |
| Temperature $T$ | 300 K |

- We will use these MC simulation results to inform the thin-film photoemission model at high field

# DFT modeling of $Cs_2Te$

- We conducted computation study of the material properties of $Cs_2Te$ needed for high field applications: structure, optical, electronic and phonons

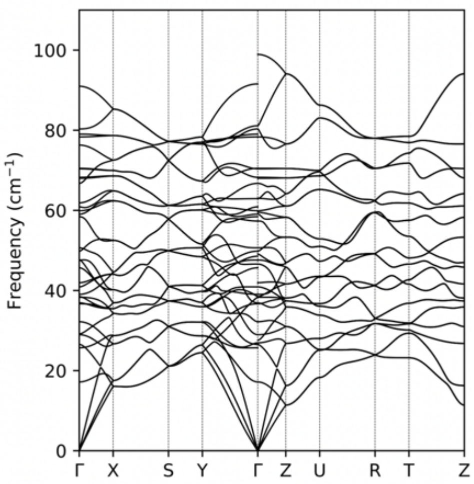


Phonon dispersion

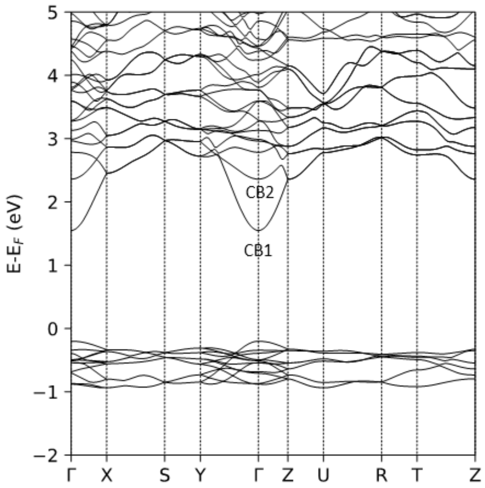


Band structure

G. Wang et al., “First-principles study of structural, elastic, electronic, transport properties, and dielectric breakdown of Cs2Te photocathode,” Sci. Rep., vol. 15, p. 2780, 2025

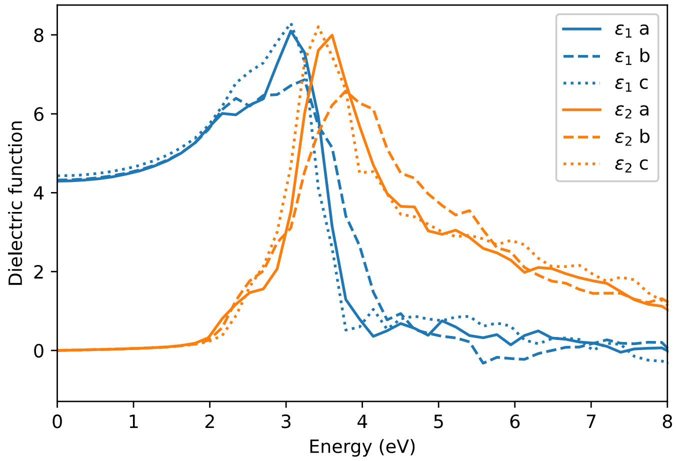


Optical properties used in the optical interference model

# Gun phase scan with semiconductor photocathodes

Space charge limited regime

Space charge during emission

source limited regime

Secondary emission

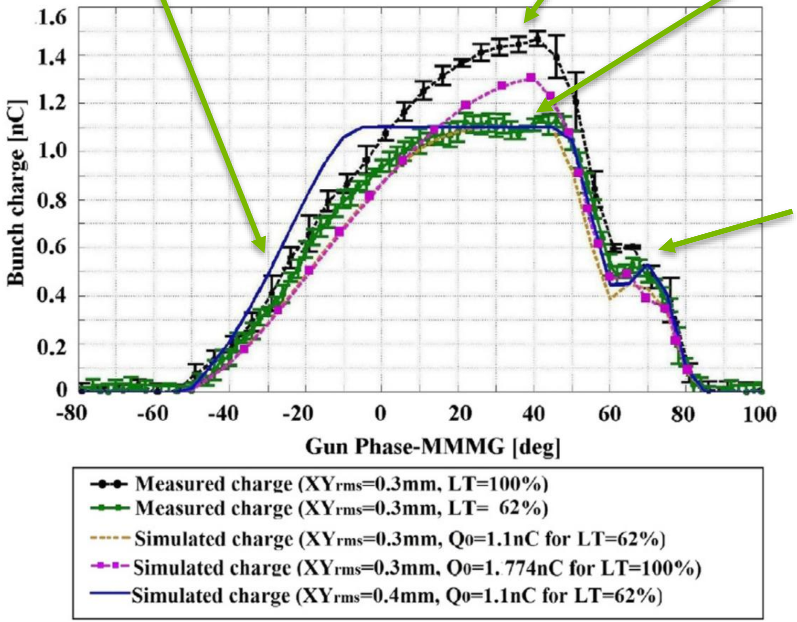


PITZ gun phase scan

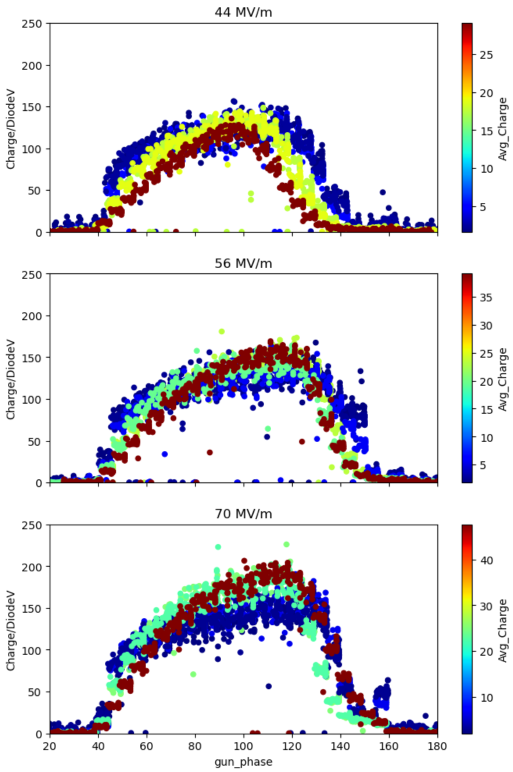


AWA gun phase scan

# Monte-Carlo calculation at high fields : enhancement from electron transport in Cs2Te*

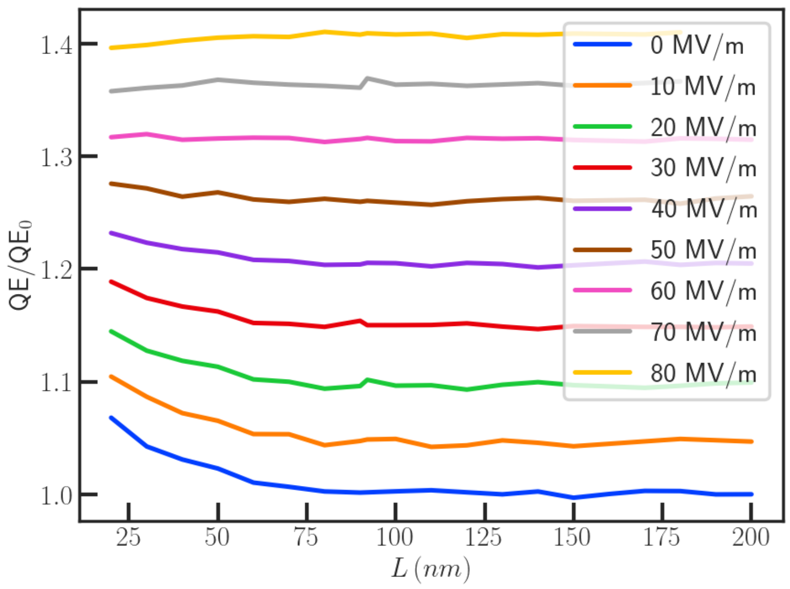


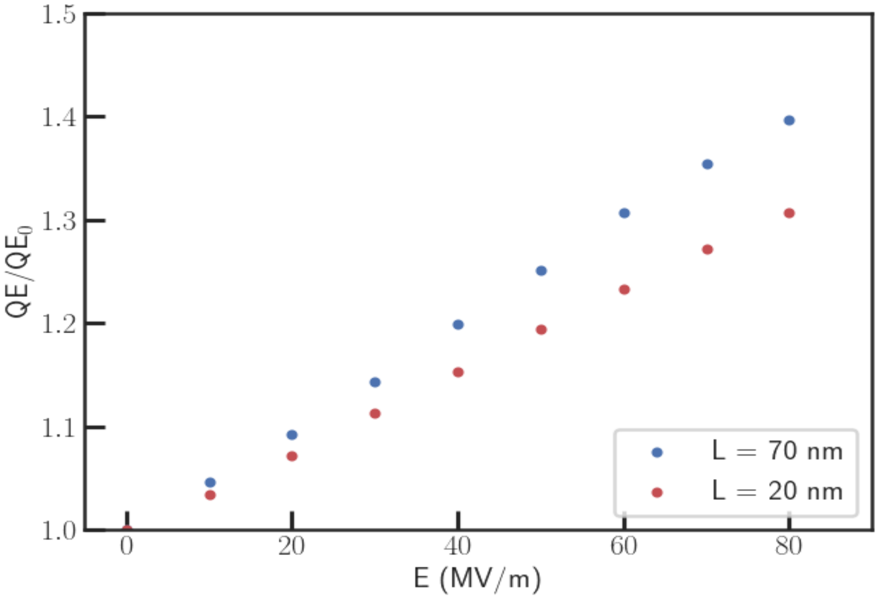


**Preliminary Results :** Effects from film thickness and gradients

* tunneling is included in the gun simulation

# Argonne Wakefield Accelerator (AWA) Facility Overview

- 3 L-band photoinjector beamlines
  - Drive beamline (this work)
  - Witness beamline
  - Argonne Cathode Test-stand (ACT)
- 1 X-band short-pulse photoinjector powered by structure wakefield acceleration

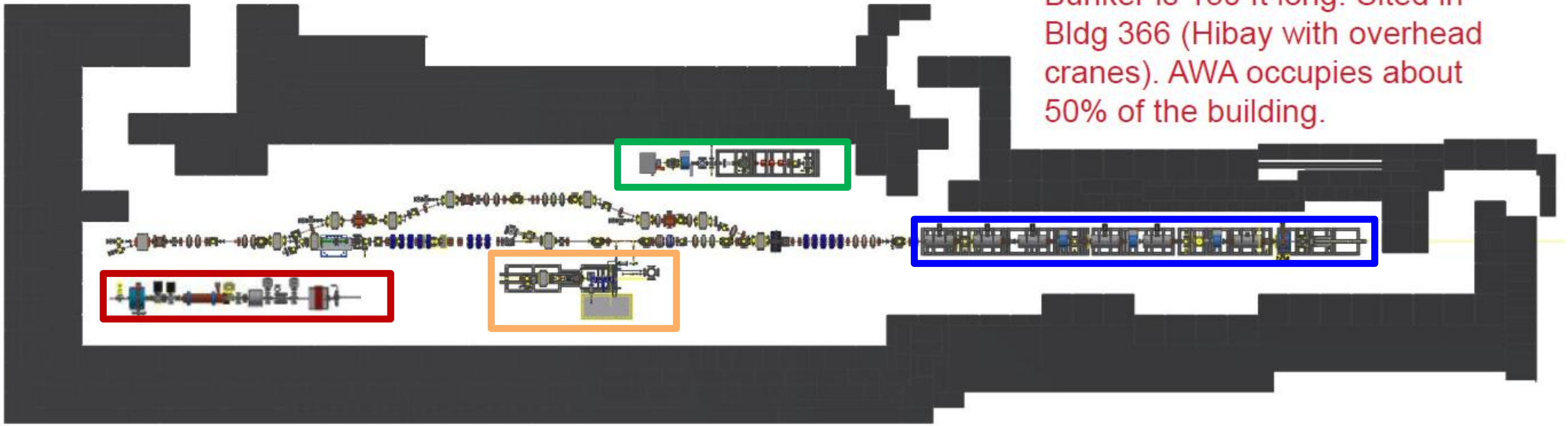

Bunker is 130 ft long. Sited in Bldg 366 (Hibay with overhead cranes). AWA occupies about 50% of the building.

# L-band drive photoinjector

- 1.5-cell, 1.3 GHz photogun with a 31 mm (diameter) **$Cs_2Te$ cathode**
  - Laser wavelength 262 nm, laser pulse duration 1 to 8 ps
  - UHV load-lock chamber with a base pressure of 1.5E-10 Torr
- **High-field operation**
  - Cathode surface peak field over **80 MV/m**, RF pulse length 7.6 $\mu$s
- **Wide charge range**
  - Single-bunch operation: 100 pC to **100 nC**
  - Bunch-train operation: up to **32 bunches** in a train, up to **600 nC** total charge
  - High-charge capability is the key driver behind recent breakthroughs in **high-gradient, short-pulse** acceleration using (beam-driven) structure wakefield acceleration

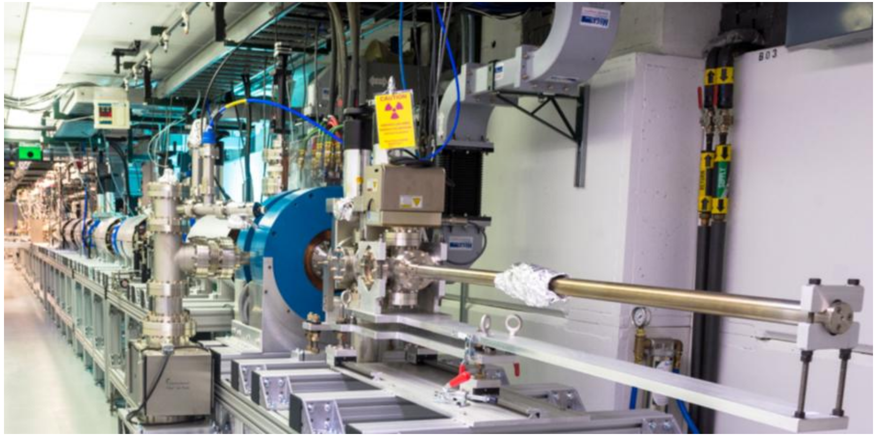

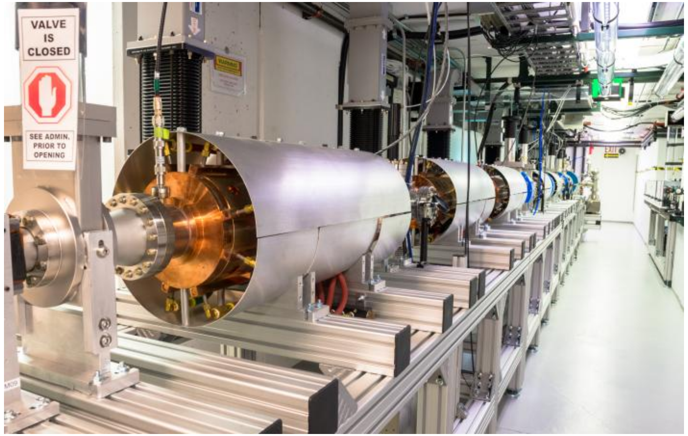

# QE measurement setup

- **Challenge #1:** closest charge monitor is not immediate after the photogun exit
  - Conducted two sets of meas. w/ linac on and off
  - Same charge measured with the linac on and off at all the gradients studied
    - Complemented with beam dynamics sims
- **Challenge #2:** large laser energy jitter
  - Photodiode measurement using leakage light

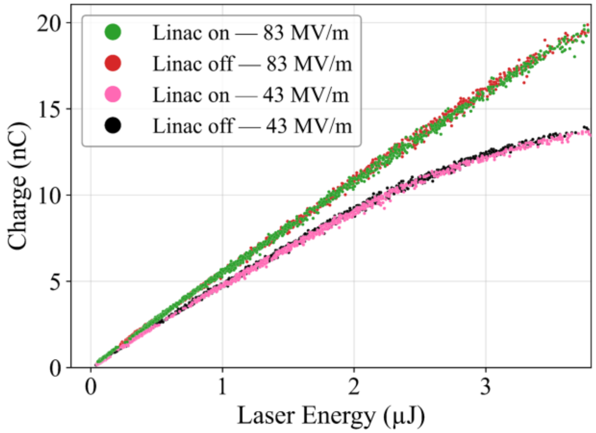


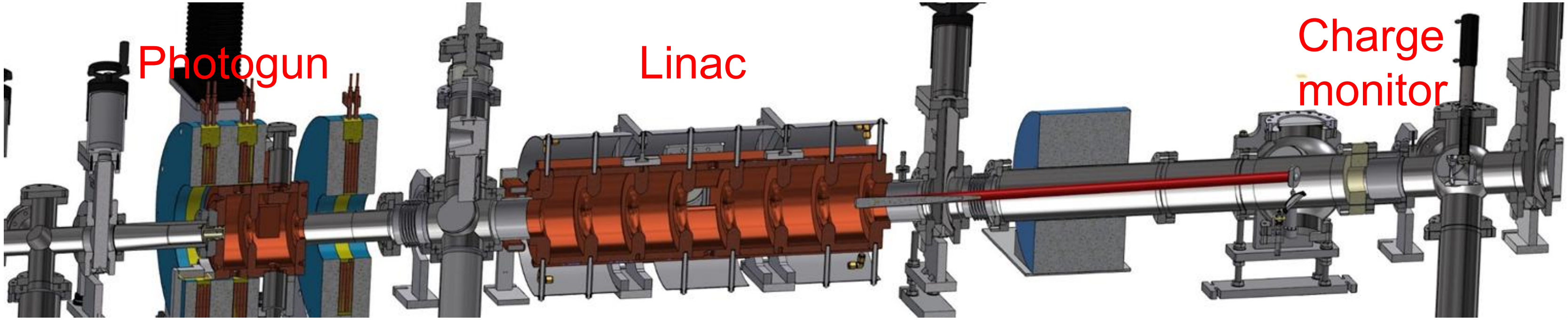

# Exp. results: QE vs. gradient

By Gaurab Rijal and AWA

- Gradient and charge scan at the nominal injector operating condition
  - RF gun = 50 deg, linac = 90 deg, laser spot size 5 mm (radius)
- Charge vs. laser energy nonlinearity at low gradient & high energy due to space charge effects
- QE increases with gradient (calculated using data in the low-charge shaded region)

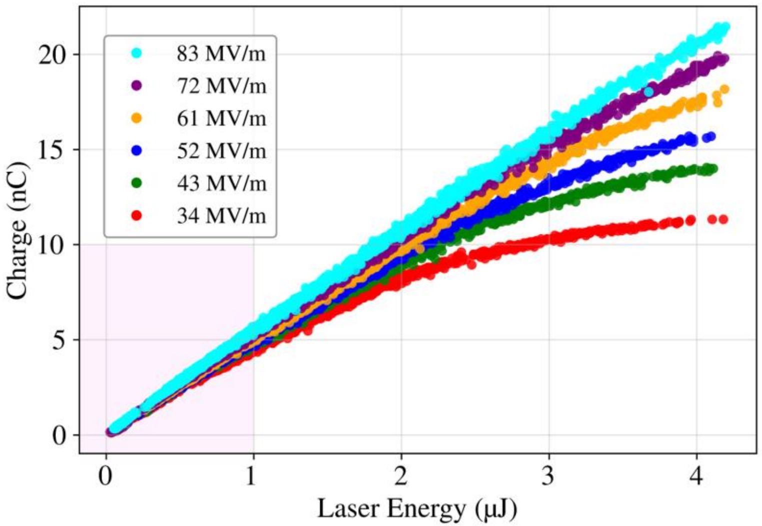


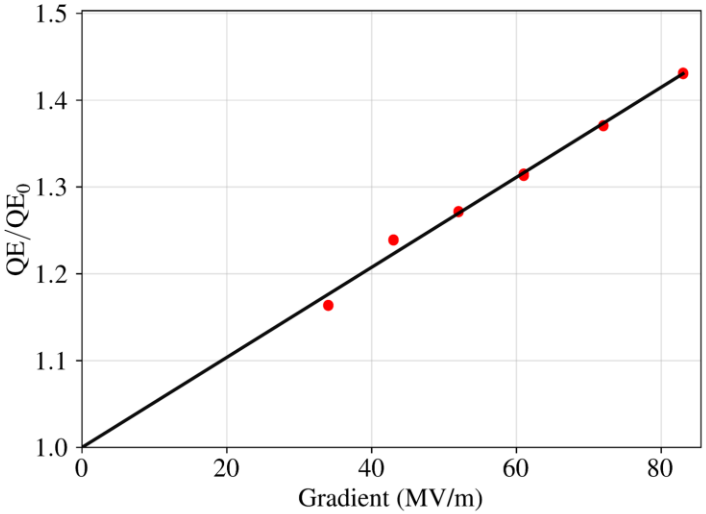

By Omkar Ramachandran

# Beam-dynamics simulations w/ MC emission model

## Code development

To simulate transport through the gun and linac, we developed a tracking code with the following features:

1. Initializes distributions using the Monte-Carlo photoemission model (incl. Schottky effect).
2. Beamline elements are modeled with 3D field-maps.
3. 3D space charge is modeled using with a rest-frame Poisson solve at each timestep.
4. Secondary electron emissions are modeled on the photocathode surface.

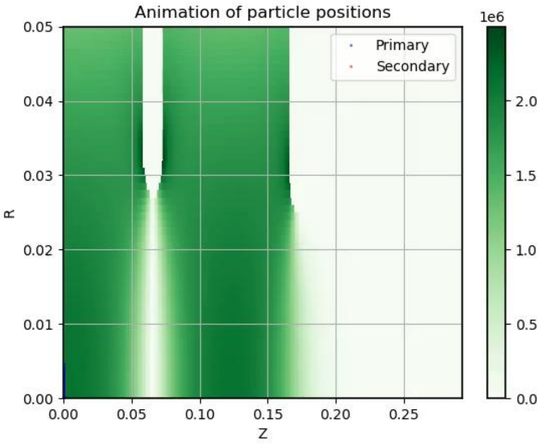


$$\delta\left(E_p\right) = \delta_{\max} \frac{E_p}{E_{p,\max}} \frac{s}{s-1+\left(\frac{E_p}{E_{p,\max}}\right)^s}$$

$$\delta_{\max} = 7.0$$

$$s = 1.5$$

$$E_{p,\max} = 2.2 \text{ eV}$$

# Beam-dynamics simulations w/ MC emission model

## Preliminary Results

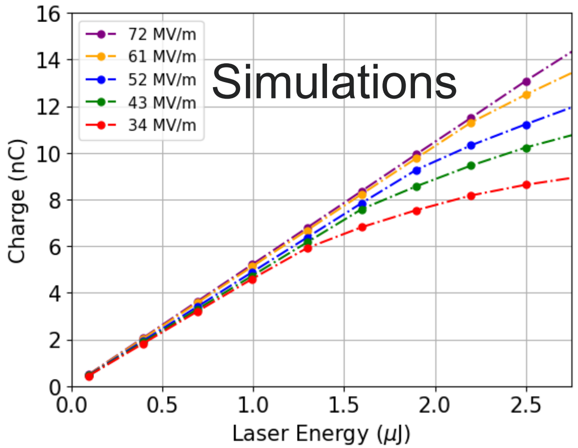


Measurement from previous slide

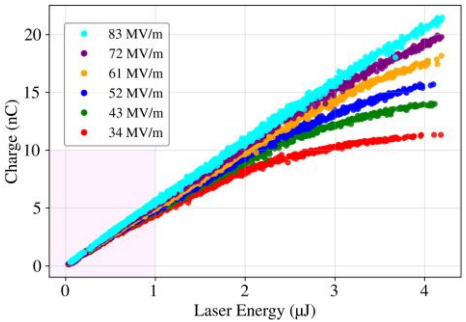


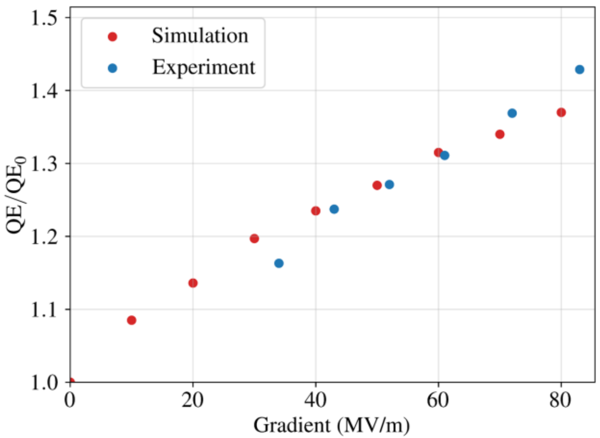


- At low gradient & high charge, space charge effect leads to beam loss at the charge monitor location.
- Beam dynamics simulations performed with distributions obtained from the MC Model predict ~40% increase from 0 to 80 MV/m.
- These results are largely in line with experimental data.

# RF phase scan at various gradient & charge

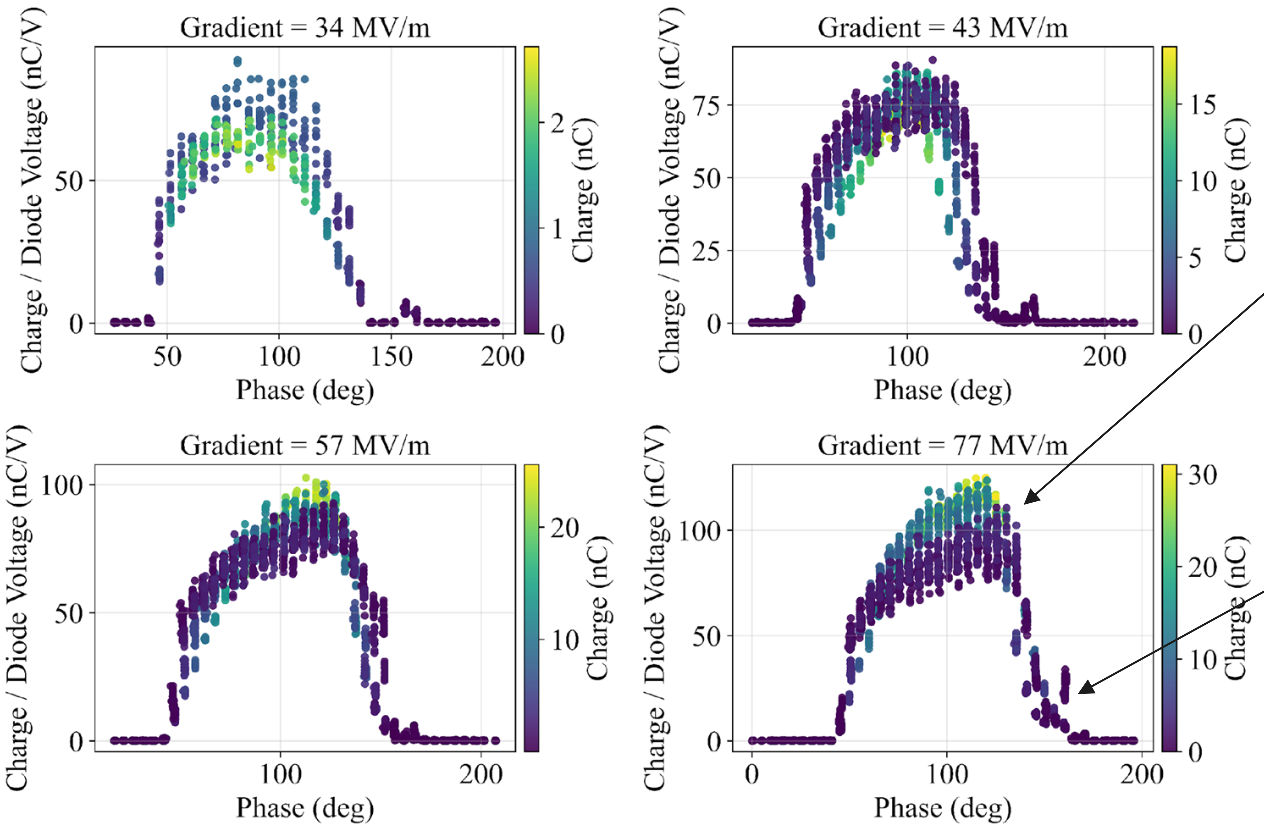


The phase scans from experiment all demonstrate the increase in charge due to QE from 0-100 deg.

All 4 gradients have secondary bumps after around 120 degrees.

# RF phase scan at various gradient & charge

## Preliminary Results

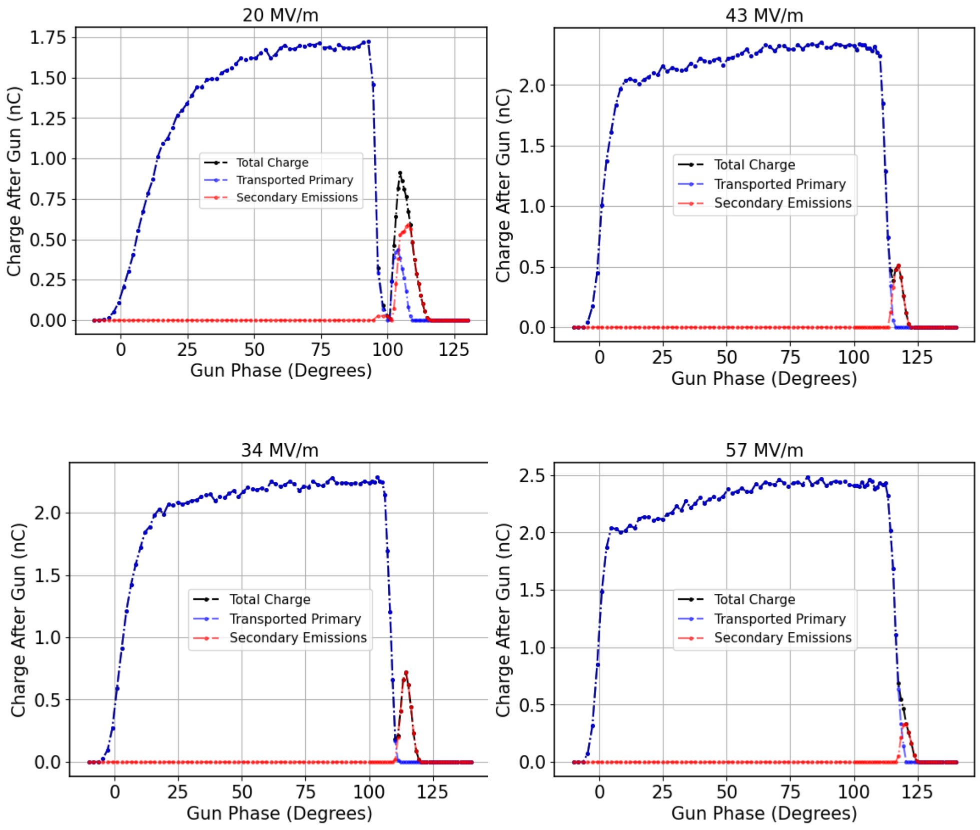


At the exit of the gun,

- The gradual increase in charge from 0-100 degrees is explained by increases in QE due to gradient.
- The bump at ~120 deg can be explained by a combination of transport and secondary emission at low gradients, and pure secondary emission at high gradients.

# X-band short-pulse photogun

- Close to **400 MV/m** measured on an X-band photocathode surface in a photogun driven by 6 ns RF pulses, **two-beam acceleration**
  - Rapid RF conditioning, low dark current, reliable operation
  - A reduction of emittance expected; detailed beam characterization in progress
- A new photogun with removable cathode plug expected in the near future
  - High-gradient cathode testing could inform other gun designs

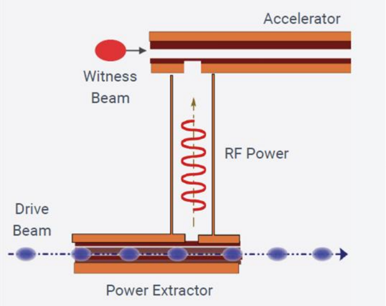


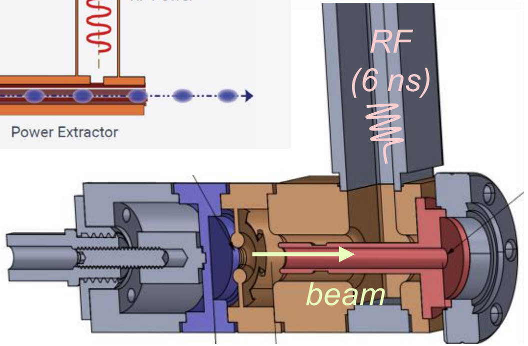


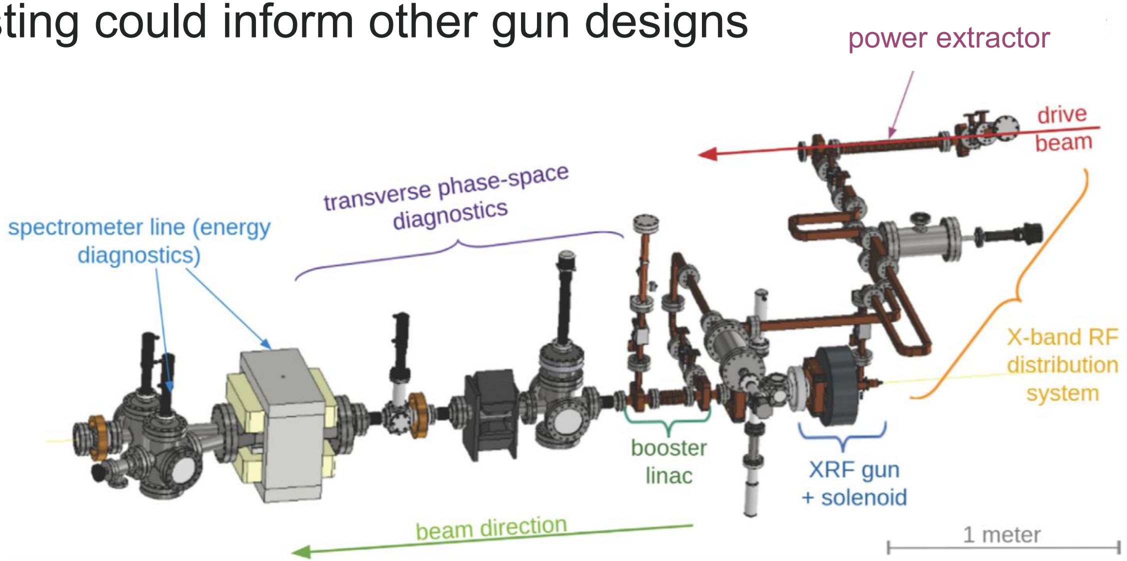

# Conclusion

- Phase-scan and $Cs_2Te$ cathode QE measurements of the AWA L-band high-field photogun are performed to characterize semiconductor-cathode behavior under various operating conditions.
- Monte Carlo and beam-dynamics simulations are compared with experimental measurements and show reasonable agreement.
- The Monte Carlo emission model can be used to study intrinsic emittance and beam brightness.
- As future high-brightness photoguns move toward even higher gradients, this approach can support their design and optimization.